ICAS 2016
30th Congress of the International Council of the Aeronautical Sciences
DCC, Daejeon, Korea ; September 25-30, 2016

ON MORE EFFECTIVE AERODYNAMIC DATA GENERATION FOR SIMULATION BASED AIRCRAFT CONCEPTUAL DESIGN

J. Park, S. Choi, and P. Raj
Virginia Polytechnic Institute & State University

KEYWORDS: ***Aerodynamics, Conceptual Design, MDO***

Abstract

Aircraft manufacturers continue to face the overwhelming challenge of developing quality aircraft at affordable cost. Traditional design practices, which rely on extensive experimental testing to generate data for configuration design and on developing physical prototypes to verify functional and operational characteristics, cannot effectively tackle this challenge. Simulation based design (SBD) offers a more promising avenue. It combines the ever increasing power of computers with increasingly developed modeling and simulation technologies. SBD uses high-fidelity computational methods to produce a virtual prototype which can faithfully represent the functional and operational characteristics of the real airplane to be built. SBD is implemented using multidisciplinary analysis, design and optimization (MADO) frameworks. High-fidelity computational fluid dynamics (CFD) methods are almost exclusively used to generate the required aerodynamic data. For flow conditions where even the high-fidelity CFD does not generate credible data, a Tightly Coupled Test and Computations (TiCTaC) approach is presented in this paper. It judiciously combines CFD and wind tunnel test (WTT) results to more effectively generate the required aerodynamic data.

1 Introduction

From the very inception of flight, both military and commercial aircraft have exhibited dramatic escalation in cost that has gone hand-in-hand with phenomenal improvements in performance. For example, the U.S. combat aircraft unit cost has grown by a factor of four every 10 years—a highly undesirable trend which, if remained unchecked, will render aircraft totally unaffordable in the future [1]. It is safe to conclude that *affordability* is the overarching challenge of aircraft manufacturers.

It has been recognized for more than three decades now that reducing the total life cycle cost (LCC)—conception to disposal—is the right path to affordability. LCC is about equally split between two functions: (a) operation & support (O&S), and (b) design, test and production, the latter being the main responsibility of the manufacturers. The production cost is typically 30% to 35% of the LCC, and design & test cost is about 15% to 20% [2].

It may appear at first glance that LCC reduction is best accomplished by reducing production plus O&S costs which are 80% to 85% of LCC. However, a more critical analysis

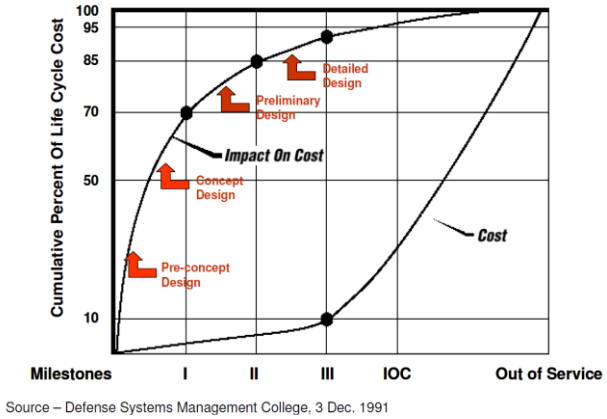

Fig. 1. Up to 70% of LCC is committed in the conceptual design stage.

suggests that focusing on design and test activities is much more desirable because they have a disproportionately large impact on LCC. As shown by the curve labeled *Impact on Cost* in Figure 1, up to 70% of the cumulative LCC is a direct result of decisions made in the early [pre-milestone I] stages of design! It is equally important to note that making design changes in the later stages gets increasingly more expensive [2]. Therefore, any effective strategy for reducing LCC must focus on design processes used in the early conceptual design (CD) phase. Meeting the aerodynamic data needs of aircraft CD in a cost-effective manner is the primary focus of TiCTaC [3].

In this paper, the authors highlight the key features of simulation based aircraft in Section 2. This is followed by a description of the mathematical formulation and preliminary results in Section 3. A few concluding remarks in Section 4 complete the paper.

2 Simulation Based Design

The very early years of aircraft design were largely dominated by a *fly-fix-fly* approach. In the 1920s and 1930s, rapid advances in aeronautical sciences produced analysis and ground test methods that could be used to systematically guide aircraft design. Consequently, the probability of achieving desired performance objectives increased. The process that evolved to implement this approach is termed the "traditional design process" in this paper.

2.1 Traditional Design Process

The traditional design process is typically carried out in three stages: conceptual, preliminary and detail. In each stage, the myriad of activities falls into two categories: synthesis and analysis. Synthesis, performed by design groups, covers defining and altering concepts to meet customer requirements. Analysis, performed by groups of disciplinary specialists, encompasses methods, tools and expertise to produce data and its use in evaluating candidate concepts.

In a traditional design process, the amount of resources (human, material and financial) allocated to conceptual design is typically quite small, of the order of 1%, as shown in Figure 1. Most of the decisions are, therefore, based on data from relatively crude and simplistic analyses and tests using tools that are fast and cheap. Also, manufacturing, operation and support functions are incorporated into decision making in a rather superficial way, if at all, due to time and cost constraints. This approach loses sight of the crucial fact that *decisions made in the early stages essentially define the fundamental architecture of the airplane* and largely dictate how it will have to be manufactured, operated and supported—and hence determine the LCC [2].

2.2 The SBD Process

A simulation based design (SBD) process employs integrated multi-disciplinary models, computational simulations and simulators to guide the development of a virtual prototype (VP) with a degree of functional realism comparable to a physical prototype. In contrast, a traditional design process focuses on producing physical prototypes to validate the functional characteristics of the design.

SBD replaces the traditional design process with one characterized by simultaneous or concurrent consideration of *all* aspects of aircraft development including engineering, manufacturing, maintainability, operations, etc. It relies on considering all requirements and constraints *from the start* rather than altering a design in its later stages to facilitate manufacturing or accommodate product support needs. Proper trade-offs can be made in *early stages of design* and the need for design changes later on is considerably reduced. As shown in Figure 2, the SBD process is targeted at substantially increasing knowledge about design and freedom to change designs in the early stages as compared to the traditional design process.

The SBD process is enabled by integration of computer-aided methods for design, engineering, manufacturing, etc. The CAD (computer-aided design), CAE (computer-aided engineering) and CAM (computer-aided manufacturing) methods have been in use for quite some time now. However, they have been exercised in relatively segregated environments.

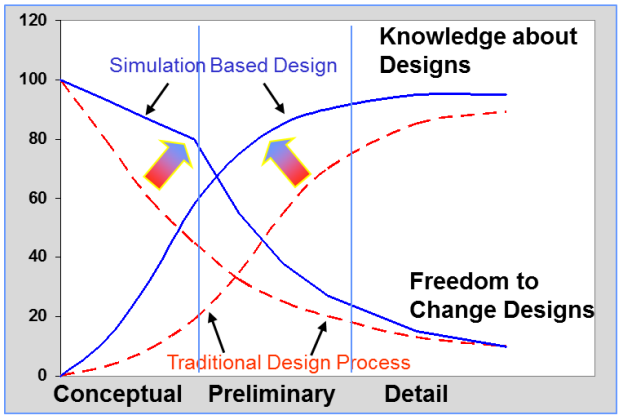

Fig. 2. SBD increases knowledge about designs and freedom to change design in early stages

Each engineering group typically maintains its own geometric models and data formats. When interacting with other groups, much extra effort is required to reconcile geometric and data incompatibilities. This process is fraught with potential for errors and delays. This problem is alleviated through a Virtual Prototype Database which maintains all design information digitally, as shown schematically in Figure 3. The challenge is to ensure that data supplied by the various groups conform to the database standards. The product definition database must not only support the needs of the design community, but also be useable for modeling & simulation activities of other communities including acquisition, logistics, and operations.

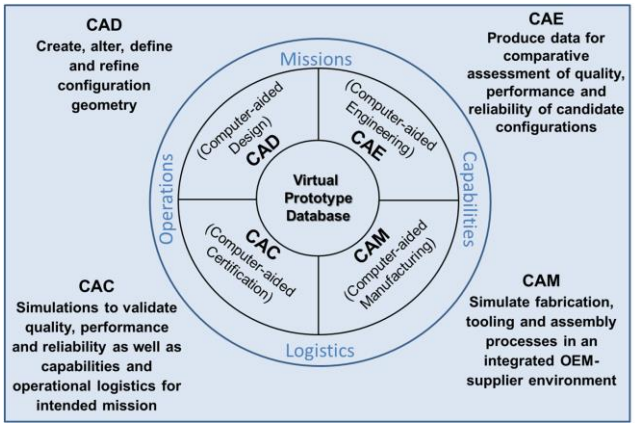

Fig. 3. SBD process is enabled by efficient integration of computer-aided methods

For effective integration of computational simulation methods, multidisciplinary analysis, design and optimization (MADO) frameworks have been developed [4,5] which execute an integrated multidisciplinary design process. The frameworks facilitate integration of computational simulation modules of disciplinary specialties including design, engineering, manufacturing, cost, etc., along with computational optimization modules to conduct design trades.

2.3 Role of CFD in SBD

CFD is an indispensable tool for SBD due to two principal reasons. First, CFD methods have been proven to computationally simulate flow about complex configurations to generate the required aerodynamic data such as forces and moments and stability & control parameters needed to evaluate airplane performance. Such evaluations are essential to ensuring that the final configuration would be able to successfully carry out the intended mission. Second, CFD provides critical input data for many other CAE methods. For example, airframe structural analysis requires steady and unsteady loads that CFD can provide. Flight control system design requires airplane response to control commands; CFD provides incremental forces and moments. In addition, CFD can provide on- and off-body data for an improved understanding of the flow features surrounding an airplane which offers valuable guidance for modifying the configurations.

Note that wind tunnels have traditionally provided the types of design data that SBD demands of CFD. However, traditional wind tunnel tests are not well suited for meeting the demands and tempo of a SBD process. Evaluating a large number of design variations (dozens not a few) in a short period of time (hours or days not weeks and months) is expected in a SBD study. Also, it is crucial that every successive design incorporate the learning from the preceding designs. CFD holds an edge over wind tunnels in meeting this expectation. The time and cost of building a large number of wind tunnel models and conducting a large number of tests are prohibitive in comparison to using CFD.

A wide variety of CFD methods are now available to support aircraft design needs. The methods range from the “low-fidelity” vortex-lattice and panel codes based on the linear potential equations to “high-fidelity” Reynolds-averaged Navier-Stokes (RANS) codes. The

"fidelity" qualifier directly relates to the level of simplifying assumptions made in deriving the governing equations of flow physics. Note that Large-Eddy Simulation (LES) and Direct Numerical Simulation (DNS) codes offer more sophisticated representations of flow physics. However, only RANS codes have made inroads into aircraft design because LES and DNS place severe demands on computational resources by comparison.

Although the time and cost of CFD simulations keep reducing with each passing year, assessing credibility of predictions remains an overarching challenge. When using the RANS codes, lack of credibility of predictions is a direct consequence of inadequacies of turbulence models, especially for flows with significant regions of separation. Sample results are included here for an uninhabited combat configuration, SACCON [6], shown in Figure 4.

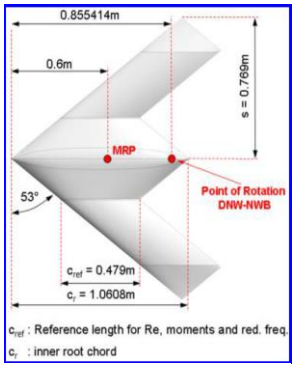

Figure 4. Planform and geometric parameters of SACCON [6]

Sensitivity of predicted lift and pitching moment coefficients to turbulence models is shown in Figure 5. The computed solutions for 0.149 Mach number and 1.6 million Reynolds number were generated using the NASA USM3D RANS code—a state-of-the-art unstructured-grid CFD method—with a grid containing more than six million tetrahedra. Correlations with wind-tunnel data clearly show that the RANS predictions are less than satisfactory especially for pitching moment.

In general, experiences with RANS simulations of turbulent flows have been mixed. There have been many successes with rather simple models and many failures with the more sophisticated ones depending on the complexity of the flow field. Attempts at refining existing models and developing new ones continue unabated. In the authors' opinion, the prospects of a universal turbulence model are rather bleak; representing the complexity of turbulent flows using a model with a few free parameters is a long shot indeed [2].

3 TiCTaC Development

TiCTaC is mainly targeted at meeting the aerodynamic data needs of MADO-based conceptual design efforts [3]. As discussed in Section 1, the impact of decisions made in the CD stage have far-reaching consequences for the overall life cycle cost. Therefore, it is imperative that credible data be used to make more informed decisions. Instead of relying entirely on CFD methods, authors are exploring the best ways of judiciously coupling the CFD and wind-tunnel tests (WTTs). The premise is: WTTs provide the highest fidelity data for all types of flows. The RANS CFD methods are quite capable of

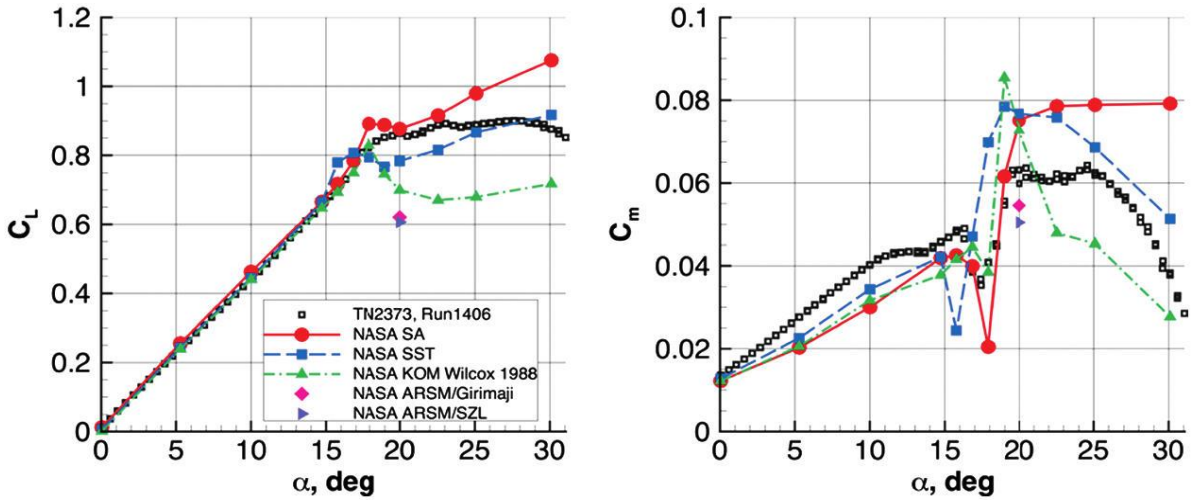

Figure 5. Sensitivity of C_L and C_m values computed using NASA USM3D to turbulence models [6]

providing high-fidelity data for attached and mildly separated flows, and the low-fidelity panel codes are good for attached flows except at transonic conditions.

3.1 Objectives

The three principal objectives are:

- To produce credible aerodynamic data, regardless of the source, that meets the needs of aircraft CD using MADO.
- To explore the best way of coupling CFD and WTT results to generate credible data.
- To make sure that the resulting system is more cost-effective than other approaches.

3.2 Framework for TiCTaC Development

To achieve the objectives in Section 3.1, the MADO framework shown schematically in Figure 6 is being used to guide further development and demonstration of TiCTaC. The key constituents of this framework are (i) the Variable-Fidelity (VF) surrogate model with low-accuracy sample point filtered by the consideration of physical errors; (ii) infill sample criteria; and (iii) fidelity indication by an overlapping coefficient (OVL).

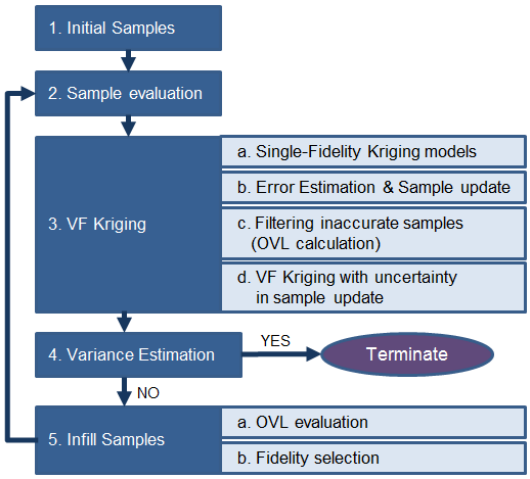

Figure 6. An MADO framework incorporating TiCTaC for generating aerodynamic data

The basic premises are:

- WTTs provide the highest fidelity data for all types of flow.
- The high-fidelity RANS CFD methods are capable of providing high-fidelity data for attached and mildly separated flows. In many cases, Euler CFD codes can be quite effective as well.
- The low-fidelity (linear potential) panel method is effective for attached flows, except under nonlinear transonic conditions.

First, initial sample points for each fidelity are selected in Step 1 based on Latin Hypercube Sampling (LHS) by varying design variables with certain bounds. In this step, more low-fidelity samples and fewer high-fidelity samples are chosen to save cost and time. In Step 2, the function value is calculated for each sample point. With the function values computed by the variable fidelity analysis methods, a Kriging surrogate model is generated in Step 3.

For the VF Kriging model, a single-fidelity (SF) Kriging model [8] for each fidelity sample set is first made. Based on this SF Kriging model, error terms of each fidelity sample are estimated. The error terms are used to update the fidelity of sample points. An overlapping coefficient [9] is used to filter out the updated sample points that have low accuracy. The OVL checks the closeness of function values of the lower fidelity sample points with the highest fidelity samples. If the function value of the lower fidelity sample is not close to that of the highest fidelity sample, i.e., the lower fidelity sample is off-trended, these lower fidelity samples are filtered and not used to construct the variable-fidelity Kriging model. The updated lower fidelity samples also have physical errors that are separate from the sampling errors which are taken into account by the ordinary VF Kriging method. The VF Kriging model in the current study considers uncertainty from both the distribution of sample points and the inaccuracy of lower fidelity samples. Next, the variance of Kriging estimation is updated with the physical errors of the lower-fidelity samples. This makes the framework in the present study more accurate with less number of sample points than the ordinary VF Kriging model.

Once the VF Kriging surrogate model is generated, the global accuracy of the model is checked in Step 4 by estimating the variance values of Kriging predictions at several trial locations. If the highest variance of surrogate model is lower than a certain criterion, the framework is terminated. Otherwise, more

sample points are needed at the trial locations with high variance value, and the OVL becomes the fidelity indicator in Step 5. The suitable fidelity is selected based on the overlapping coefficient. The relevant mathematical details of each step are presented in Section 3.3.

3.3 Mathematical Formulation

Single-fidelity Kriging surrogate models are first generated for each of the fidelity methods using the selected initial sample points. Then, based on the estimated function values of each Kriging model, error terms are evaluated. In this paper, for M number of different fidelity methods, the error terms of each fidelity model are defined in Eq. (1).

$$\begin{aligned} F_{1,j} &= \alpha_1 F_{2,j} + \beta_{1,j} \\ &\vdots \\ F_{i,j} &= \alpha_i F_{i+1,j} + \beta_{i,j} \\ &\vdots \\ F_{M-1,j} &= \alpha_{M-1} F_{M,j} + \beta_{M-1,j} \\ F_{M,j} & \end{aligned} \tag{1}$$

In Eq. (1), F is the function value of each fidelity method, i is the index of fidelity, and j is the index of arbitrary sample location in the design space. Note that higher the i index, higher the fidelity. α_i is the multiplicative error of the i^{th} fidelity method, and its value depends on the accuracy of the source of data. $\beta_{i,j}$ is the additive error term of i^{th} fidelity method at j^{th} location. The additional error term depends on both accuracy of the model and the location of data in the design space. It is assumed that the highest-fidelity sample has the exact value because it is the most accurate data that is available.

For evaluation of the error term, Eq. (1) can be written in a matrix form. For example, the equation can be written as Eq. (2) for three different fidelity methods ($M = 3$). This equation is shown for additive error vector. In Eq. (2), $\hat{F}_{i,j}$ is the function prediction of single-fidelity Kriging model by the i^{th} fidelity sample data at the j^{th} location, and c is the index of the highest fidelity (3rd) sample location.

$$\begin{bmatrix} \beta_{1,c} \\ \beta_{2,c} \end{bmatrix} = \begin{bmatrix} 1 & \alpha_1 \\ 0 & 1 \end{bmatrix}^{-1} \begin{bmatrix} \hat{F}_{1,c} - \alpha_1 \alpha_2 F_{3,c} \\ \hat{F}_{2,c} - \alpha_2 F_{3,c} \end{bmatrix} \tag{2}$$

Now, using genetic algorithm, a sub-optimization problem is solved for α_i which makes the norm of β vector a minimum. The purpose of this process is to fit certain lower fidelity data to the highest fidelity data with the minimum additive error. Once the multiplicative errors are found, the additive error vector can be calculated with the highest-fidelity sample point. While generating the Kriging model with additive error vector, the additive error of each fidelity model at an arbitrary point, $\hat{\beta}_{i,j}$, can be estimated. These error terms are used to update the original sample data. Substituting the error terms into Eq. (1), the updated function value can be estimated. For three different fidelity methods, the function values of the two lower fidelity samples can be updated using Eqs. (3) and (4).

$$F'_{1,j} = \frac{F_{1,j} - (\hat{\beta}_{1,j} + \alpha_1 \hat{\beta}_{2,j})}{\alpha_1 \alpha_2} \tag{3}$$

$$F'_{2,j} = \frac{F_{2,j} - \hat{\beta}_{2,j}}{\alpha_2} \tag{4}$$

Because each additive error term is estimated from the Kriging surrogate model, $F'_{1,j}$ and $F'_{2,j}$ have stochastic values which follow the Gaussian distribution. By comparing the probability distribution of updated samples and the probability distribution of highest fidelity sample, appropriate samples for variable-fidelity Kriging model can be filtered with OVL. The overlapping coefficient of the 2nd lowest fidelity method at each sample point can be defined as Eq. (5).

$$OVL_{2,b} = \int_{R_n} \min\left(p_{2,b}(x), p_{M,b}(x)\right) dx \tag{5}$$

In Eq. (5), b is the index of the 2nd lowest fidelity sample location. $p_{2,b}(x)$ and $p_{M,b}(x)$ are the probabilities of the updated 2nd lowest fidelity sample at the b^{th} location, and of the highest fidelity (M) sample at the b^{th} location respectively. Sample data with an OVL value greater than a certain criterion are selected and used for the variable-fidelity Kriging model.

Once the sample data are selected, the Kriging model is generated. Because lower fidelity sample data are updated with stochastic process, the uncertainty of lower-fidelity sample should be considered. In this study, the ordinary

Kriging estimation is updated with the uncertainties of updated sample data. Eq. (6) shows the equation for Kriging model [10,11]

$$\hat{F}_{VF} = \mu + g + \varepsilon, \qquad g \in \mathbb{N}(0, \sigma_{VF}^2) \qquad (6)$$

In Eq. (6), $\hat{F}_{VF}$ is the estimated function value of variable-fidelity Kriging, μ is the mean value of function value, σ_{VF}^2 is the variance of Gaussian distribution, and ε is the uncertainty of sample data values due to its physics model. ε follows the Gaussian distribution whose mean value is 0 and variance is τ^2.

Next, the ordinary Kriging model is generated with the mean value of filtered sample. Eq. (7) and Eq. (8) show the predicted function values from the 2nd lower fidelity sample. $\hat{F}_{VF2,k}$ is the function prediction at the filtered sample points, and $\hat{F}_{VF2,j}$ at a new arbitrary sample points.

$$\hat{F}_{VF2,k} = \mu_{VF2,k} + g_k, \qquad g_k \in \mathbb{N}\left(0, \sigma_{VF2,k}^2\right) \qquad (7)$$

$$\hat{F}_{VF2,j} = \mu_{VF2,j} + g_j, \qquad g_j \in \mathbb{N}\left(0, \sigma_{VF2,k}^2\right) \qquad (8)$$

Using Eq. (7), Eq. (8), and ε, the mean and variance of $\hat{F}_{VF}$ at an arbitrary point is updated as shown in Eq. (9) and Eq. (10). In these equations, C_{21} is the correlation matrix between g_j and g_k, and C_{11} and C_{22} are the correlation matrix between g_j and g_j and the correlation matrix between g_k and g_k respectively.

$$Mean\ E\left(\hat{F}_{VF}\right) = \mu_{VF2} + C_{21}(C_{21} + \tau^2 I)^{-1}(F' - \mu_{VF1}) \qquad (9)$$

$$Variance\ V\left(\hat{F}_{VF}\right) = C_{22} + \tau^2 I - C_{21}(C_{11} + \tau^2 I)^{-1}{C_{21}}^T \qquad (10)$$

For determining the additional points to improve the Kriging model, the variance, Eq. (10), is checked as a measure of the global accuracy. In the ordinary Kriging, the variance indicated the sampling error which depends on the distribution of sample data. However, using the Kriging model of Eq. (6), the effect of both sampling error and inaccuracy of lower fidelity samples can be included in the variance $V\left(\hat{F}_{VF}\right)$. To improve the model, in each iteration, the sample location with high variance is selected as the additional trial location.

3.4 Preliminary Results

To demonstrate the feasibility and veracity of the TiCTaC framework (Section 3.2) and the mathematical formulation (Section 3.3), two simple test problems are considered and results are presented in this section.

3.4.1 Lift coefficient of NACA0012 airfoil

The objective is to predict the lift coefficient vs. angle of attack curve of NACA 0012 airfoil using data from three different fidelity methods: panel method, RANS method, and wind tunnel test. The flow condition are: M = 0.089 and Re = 2.0×10^6. The wind tunnel data of Reference 12 is used. The number of initial samples of panel method, RANS method, and wind tunnel test are set at 10, 5, and 4 respectively. Fig. 7 shows the location of the initial sample data and the corresponding lift coefficient values.

Following the MADO framework introduced in Section 3.2, the additive and multiplicative errors of each lower fidelity dataset are calculated, and the lift coefficient values of panel and RANS methods are updated.

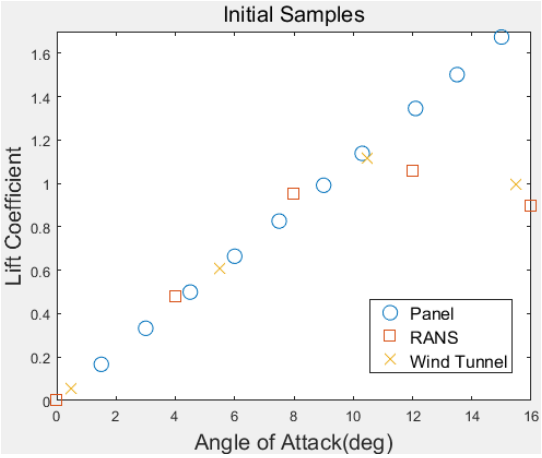

Figure 7. Initial samples for the prediction of the lift coefficient curve of NACA0012 airfoil

OVLs are calculated next and the values are shown in Fig. 8. Note that the OVL of updated panel method samples are high at low angles of attack, which means that these data can be used for the variable fidelity Kriging. However, OVL of panel method samples decreases as the angle of attack increases. Therefore, at high angles of

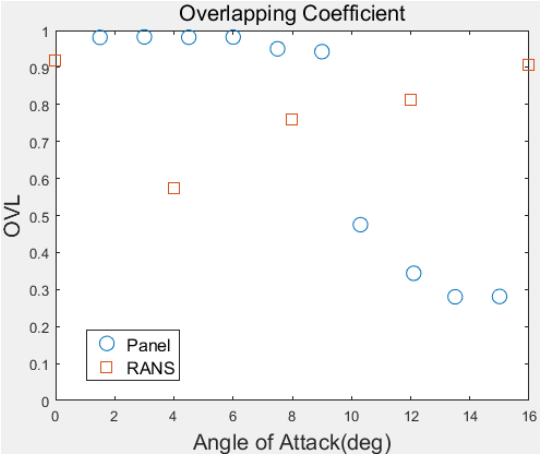

Figure 8. Overlapping coefficient of updated sample (Panel and RANS method)

attack, the panel method samples should not be used.

In Fig. 9, the variable fidelity Kriging model of the lift coefficient of the NACA0012 airfoil is compared with available wind tunnel data. the results show the discrepancy between the Kriging model predictions and the actual wind tunnel data. To improve the surrogate model, additional sample should be added. The variance of VF Kriging model is calculated as shown in Fig. 10, and it indicates that additional samples are needed at three locations based on the discrepancy shown in Fig. 9.

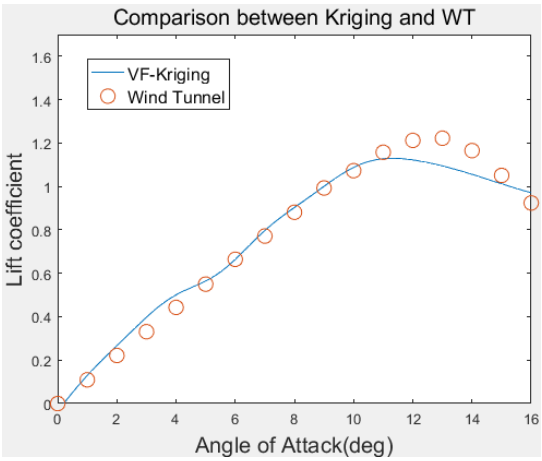

Figure 9. Variable-fidelity Kriging model of the lift coefficient of NACA0012 airfoil

3.4.2 Kriging Surrogate model with VF samples

The TiCTaC framework is applied to solve a design optimization problem using a numerical test function. Six hump camel back function [13] is selected which is one of the commonly used numerical test functions. The exact function of

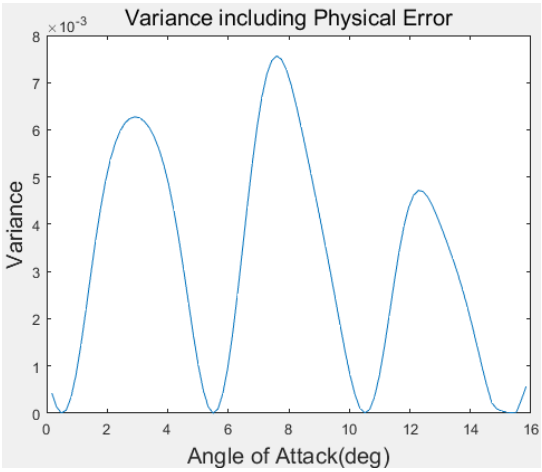

Figure 10. Variance of Variable-fidelity Kriging model of the lift coefficient of NACA0012 airfoil

six hump camel back function is shown in Eq. (13). To test variable fidelity analysis, two low fidelity numerical functions for the six hump camel back function are formed by adding artificial noise as shown in Eq. (14) and Eq. (15).

$$f(x_1, x_2) = \left(4 - 2.1x_1^2 + \frac{1}{3}x_1^4\right) x_1^2 + x_1x_2 + (-4 + 4x_2^2)x_2^2 \quad (13)$$

$$\text{, where } -2 \le x_1 \le 2, -1 \le x_2 \le 1$$

$$f_m = 1.2 \times f(x_1 + 0.05, x_2 - 0.05) + 0.3 \quad (14)$$

$$f_l = 0.7 \times f(x_1 - 0.1, x_2 + 0.1) + 0.5 \quad (15)$$

f_m represents the medium fidelity function and f_l represents the low fidelity function. The exact function is used as the highest fidelity function. The contours for all three functions are shown in Fig. 11.

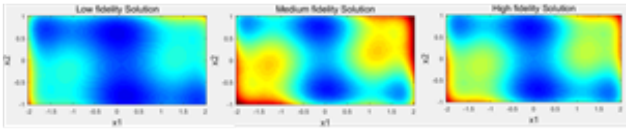

Figure 11. The contour of each different fidelity function value (Low, Medium, and high fidelity, respectively.)

At the first step, the initial sample data set is selected. For low-, medium-, and high-fidelity functions, 19, 10, and six sample points are selected respectively. Using each sample point and its function value, single fidelity Kriging model is made. Then, the multiplicative error and additive error terms are estimated, and the samples are updated. From OVL calculation, among the initial lower fidelity samples, 10 low fidelity samples and eight medium fidelity

samples are selected for the variable fidelity Kriging model. As the result, variable-fidelity Kriging model is generated as shown in Fig. 13.

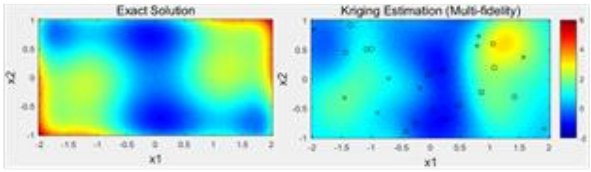

Figure 13. Comparison between the contour of exact function and the variable fidelity Kriging model at the initial optimization iteration

In this application, a modified MADO framework [7] shown in Fig. 14 is used. This involves substituting Optimization for Variance Estimation (see Fig. 6) as Step 4. For optimization, Genetic Algorithm (GA) is used. Moreover, the Multi-Objective Multi-Point Infill Sampling Criteria (MPMO-ISC) [14] is applied in Step 5.

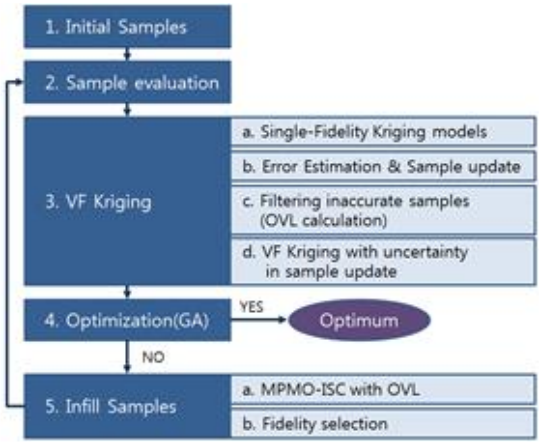

Figure 14. A modified MADO framework for optimization problem [7]

At the first design iteration, searching the minimum value with Genetic Algorithm, it is determined that additional points are needed. The additional points are selected by MPMO-ISC. Table 1 shows the history of optimization. Model error is the error between optimum value which is estimated by the design process and the exact function value at the optimum point. True error is the error between optimum value which is estimated by the design process and the optimum value which is analytically calculated. The termination criterion is set as 5%, and the process is terminated at 3rd iteration. Fig. 15 shows the comparison of contour of exact function value and the variable fidelity Kriging model at the last iteration.

Table 1. Optimization history of Numerical test

Iter.	Number of Samples			Opt.	Model error(%)	True error(%)
	Low	Med.	High			
1	19	10	6	-0.4841	116.70	53.07
2	20	10	9	-0.5325	28.48	48.38
3	21	11	10	-1.0603	3.263	2.782

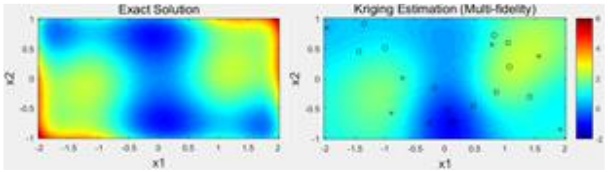

Figure 15. Comparison between the contour of exact function and variable fidelity Kriging model at the last optimization iteration.

4 Concluding Remarks

In this paper, TiCTaC approach is proposed to cost-effectively generate accurate aerodynamic data to support MADO-based conceptual design needs. A MADO framework is developed for tightly coupling CFD and wind tunnel testing, and preliminary results for simple test cases are presented to demonstrate the feasibility of the approach.

Wind tunnel testing is considered as the highest fidelity method with the highest cost. The cost of computational analysis is a function of fidelity and assumed to be lower than that of wind tunnels. The concept of variable-fidelity Kriging surrogate model is used to integrate data from computations and wind-tunnel testing. It allows filtering of sample points with low accuracy by the consideration of physical error, infill sampling criteria, and overlapping coefficient (OVL).

For preliminary verification and demonstration of the framework, the prediction of the lift coefficient curve of NACA0012 airfoil is performed with both computational and experimental data. Moreover, an optimization problem using a numerical test function is solved as a validation case. The results show that the proposed MADO framework can work efficiently for surrogate based optimization problems. Additional studies with more realistic

test cases are planned to further develop and mature the TiCTaC system.

References

[1] Augustine, N. *Augustine's Laws*, Published by American Institute of Aeronautics and Astronautics, New York, NY, 1983.

[2] Raj, P. Aircraft Design in the 21st Century: Implications for Design Methods (Invited). *29th AIAA Fluid Dynamics Conference*, Albuquerque, NM, AIAA Paper 98-2895, 1998.

[3] Raj, P, Choi, S. TiCTaC: an innovative paradigm for aerodynamic data generation to meet aircraft conceptual design needs. *RAeS Applied Aerodynamics Conference*, Bristol, UK, Paper C.3, 2016.

[4] Gur, O, Bhatia, M, Mason, W, Schetz, J, Kapania, R and Nam, T. Development of a Framework for Trussed-Braced Wing Conceptual MDO. *Structural and Multidisciplinary Optimization*, Vol. 44, No. 2, pp. 277-298, 2011.

[5] Allison, D, Morris, C, Schetz, J, Kapania R, Sultan, C, Watson, L, Deaton, J, Grandhi, R. A Multidisciplinary Design Optimization Framework for Design Studies of an Efficient Supersonic Air Vehicle. *12th AIAA Aviation Technology, Integration, and Operations (ATIO) Conference and 14th AIAA/ISSM Multidisciplinary Analysis and Optimization Conference*, Indianapolis, IN, AIAA 2012-5492, 2012.

[6] Frink, N, Tormalm, M, and Schmidt, S. Three Unstructured Computational Fluid Dynamics Studies on Generic Uninhabited Combat Air Vehicle. *AIAA Journal of Aircraft*, Vol. 49, No. 6, pp 1619-1637, 2012.

[7] Park, J., Jo, Y., Yi, S., Choi, S., and Raj P. Variable-Fidelity Multidisciplinary Design Optimization for Innovative Control Surface of Tailless Aircraft. *Aviation 2016*, Washington D.C, AIAA 2016-3573, 2016.

[8] Lophaven, S, Nielsen, H, and Søndergaard, J. DACE, A Matlab Kriging Toolbox, Informatics and Mathematical Modeling. Technical Report IMM-TR-2002-12, Technical University of Denmark, 2002.

[9] Inman, H, and Bradley, E. Jr. The overlapping coefficient as a measure of agreement between probability distributions and point estimation of the overlap of two normal densities. *Communications in Statistics - Theory and Methods*, 1989.

[10] Paciorek, C. Technical Vignette 3: Kriging, interpolation, and uncertainty. Department of Biostatistics, Harvard School of Public Health, Jan. 2008

[11] Cressie, N. *Statistics for Spatial Data*. Wiley-Interscience, New York, 1993.

[12] Kirke, B, and Lazauskas, L. Enhancing the performance of a vertical axis wind turbine using a simple variable pitch system. *Wind Engineering*, 15(4):187–195, 1991.

[13] Dixon, L, and Szego, G. The optimization problem: An introduction. *Towards Global Optimization II*. Dixon, L. C. W. and Szego, G. P. (Eds.), New York: North Holland, 1978.

[14] Yi, S, Kwon, H, and Choi, S. Efficient Global Optimization using Multi-point and Multi-objective Infill Sampling Criteria. *52nd Aerospace Science Meeting*, National Harbor, Maryland, AIAA 2014-0898, 2014.

Contact Author Email Address

mailto: schoi1@vt.edu

Copyright Statement